Spatial memory consolidation during REM sleep requires stabilization of newly formed place cells.

Richard Boyce[1†], Hyun Choong Yong[2], James E Carmichael, Mark P Brandon[3], Sylvain Williams[3†]

[1]INMED, INSERM, Aix Marseille Univ, France.

[2] Integrated Program in Neuroscience

[3] Department of Psychiatry

McGill University, Montreal, QC, Canada

†To whom correspondence should be addressed. E-mail: rboyce54@gmail.com; sylvain.williams@douglas.mcgill.ca

Abstract

The neural mechanisms behind the role of rapid-eye-movement sleep (REMs) in spatial memory formation are unclear. Here, we performed hippocampal CA1 single-unit recordings in mice expressing archaerhodopsin in GABAergic neurons of the medial septum (MSGABA), an established optogenetic method enabling REMs-selective theta rhythm attenuation resulting in spatial memory deficits. Analysis of CA1 neural assemblies during REMs revealed reduced synchrony of constituent neural activity during MSGABA silencing. Subsequent investigation of recently formed CA1 place cells demonstrated that REMs-selective MSGABA inhibition reduced the place stability of those which participated in prior REMs assembly activity, but not of those which did not. This suggests that CA1 neural assemblies during REMs facilitate spatial memory formation by stabilizing spatial representations in a plastic subpopulation of participating CA1 neurons.

Introduction

Research completed during the last several decades has produced much evidence connecting rapid-eye-movement sleep (REMs) to memory formation in human (*1-5*) and non-human models (*6-9*). Recently, a direct causal relationship between REMs and spatial memory formation was demonstrated for the first time (*10*). However, the neural mechanisms behind the role of REMs in spatial memory formation are unclear.

The ~7 Hz theta rhythm is a key feature of REMs in mice and rats which has previously been mechanistically linked to hippocampus-dependent spatial memory formation (*11-13*), although a direct link to spatial memory performance has yet to be established for these potential mechanisms. We aimed to address this issue by performing single-unit tetrode recordings in area CA1 of mice expressing archaerhodopsin (ArchT) in medial septum GABAergic neurons (MSGABA), an established optogenetic method allowing for precise inhibitory control over the memory-associated theta rhythm occurring during REMs (*10*). This allowed us to track the activity of many CA1 place cells across all portions of an experiment in which spatial memory deficits were induced following learning via REMs-selective silencing of MSGABA.

Results

To achieve ms-precision inhibitory control over MSGABA activity, we performed intraseptal injections of a virus encoding ArchT fused to an eYFP reporter in VGAT::Cre mice (Fig. S1A.)(*14*). To gain mechanistic insight into the role of hippocampal neural activity during REMs in spatial memory formation, we subsequently silenced MSGABA during REMs occurring in a 4 h rest session interposed between the encoding and recall phases of a hippocampus-dependent spatial novel object place recognition test (*10, 14-15*) (Fig. 1A.). At the start of an experiment mice were placed into a square open field with 2 identical objects ('Object1' and 'Object2') located in randomly assigned quadrants, and then allowed 30 minutes to explore the test area. Mice were then transferred to a separate cage where they were allowed a 4 h rest period, during which sleep activity was continuously monitored via hippocampal local field potential (LFP) and electromyogram (EMG) recordings. Upon entry into REMs, MSGABA were silenced via orange light delivery to the MS transfection zone until the end of the REMs episode, at which time the light was turned off. This procedure was repeated for the entire rest session resulting in MSGABA being silenced for on average 82.6 ± 0.2 % of all REMs. While this manipulation had no effect on overall characteristics of sleep activity relative to controls (Fig. 1C.; Fig. S1C.; Table S1.), there was a significant reduction in REMs theta (4-10 Hz) band power (Fig. 1B.; Fig. S1D.). Following completion of the rest session, mice were transferred back to the open field for a 30-minute spatial memory recall test session. The test area

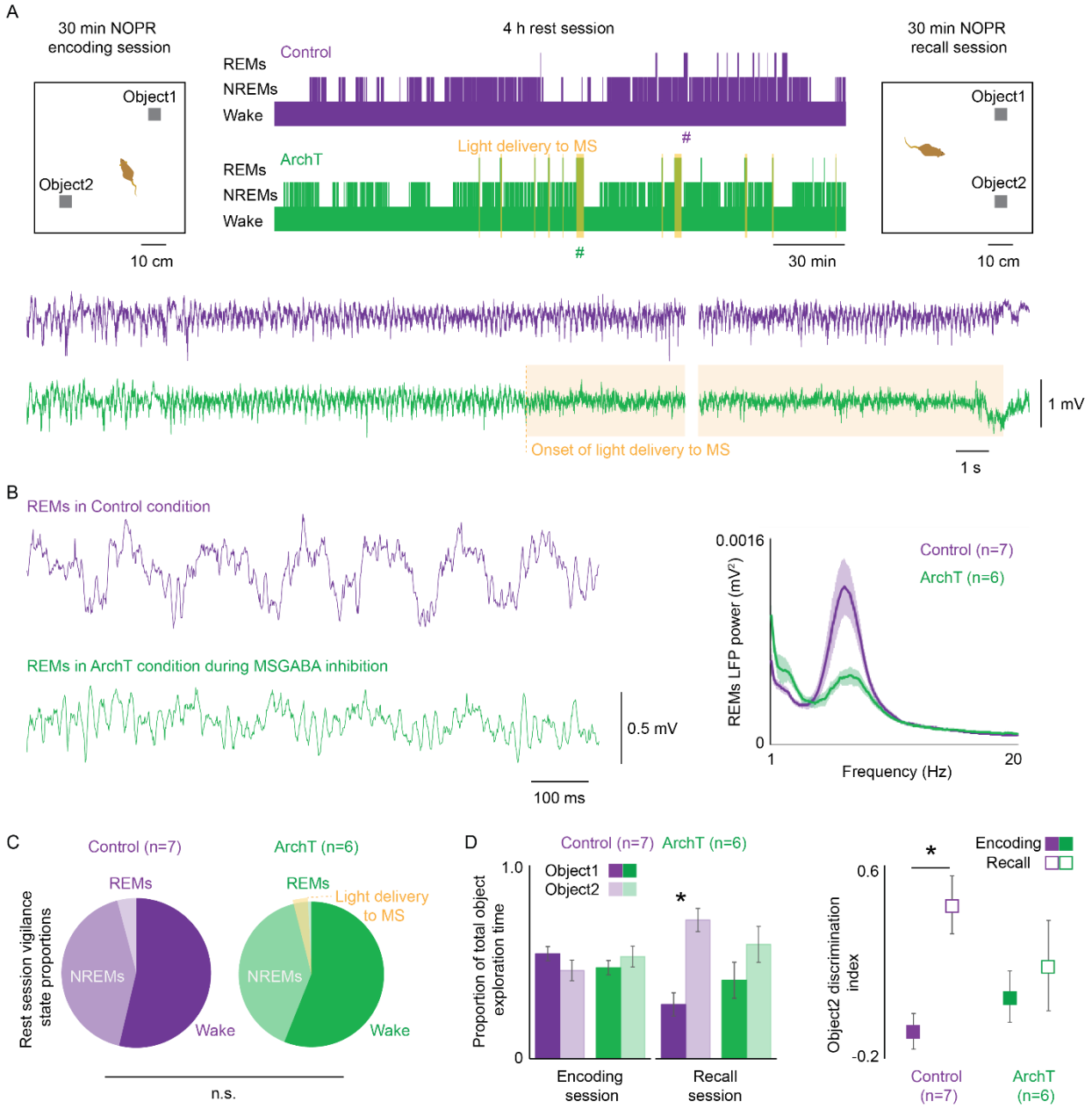
A
30 min NOPR encoding session
Object1
Object2
10 cm
4 h rest session
Control
REMs
NREMs
Wake
ArchT
Light delivery to MS
#
30 min
30 min NOPR recall session
1 mV
Onset of light delivery to MS
1 s
B
REMs in Control condition
REMs in ArchT condition during MSGABA inhibition
0.5 mV
100 ms
0.0016
REMs LFP power (mV²)
Control (n=7)
ArchT (n=6)
0
1
20
Frequency (Hz)
C
Control (n=7)
ArchT (n=6)
Rest session vigilance state proportions
REMs
NREMs
Wake
Light delivery to MS
n.s.
D
Proportion of total object exploration time
1.0
Object1
Object2
*
Encoding session
Recall session
Object2 discrimination index
0.6
-0.2
Encoding
Recall

Fig. 1. Optogenetic MSGABA silencing during REMs impairs novel object place recognition memory. (A) Schematic of behavioral experiment. Top, left. Encoding session. Top, middle. 4 h rest period during which MSGABA were optogenetically silenced selectively during REMs in the ArchT group. Top, right. Recall session. Bottom. Example traces during REMs from ArchT and Control experiments. The # symbol under hypnograms at top indicate ~ location of data segments. (B) Left. High-resolution sample traces showing the effects of MSGABA inhibition on the CA1 LFP during REMs. Right. Spectral analysis of CA1 LFP power during REMs. (C) Vigilance state proportions during the rest session. (n=7 (Control), n=6 (ArchT); n.s.=not significant, two-way ANOVA). (D) Left. Proportion of object exploration time in the encoding vs recall sessions. (n=7 (Control), n=6 (ArchT); *P<0.05, paired t-test). Right. Object2 discrimination index for the encoding vs recall sessions. (n=7 (Control), n=6 (ArchT); *P<0.05, paired t-test).

was identical to that during the encoding session, with the exception that Object2 was moved to a new location. As mice preferentially investigate novelty, the bias of a mouse for exploration of Object2 during the recall vs encoding session (Object2 discrimination index (DI)) is a metric of intact spatial memory (*15*). Mice which had MSGABA selectively silenced during REMs (ArchT mice) showed no difference in Object2 DI between the encoding and recall sessions whereas Control mice had a significantly higher Object2 DI during the recall session relative to the encoding session (Fig. 1D, right.). Cumulatively, these results therefore suggest that MSGABA activity occurring selectively during REMs is critical for hippocampus-dependent spatial memory formation, consistent with our prior report (*10*).

To interrogate potential neural mechanisms behind the observed disruption of spatial memory following REMs-specific MSGABA inhibition, we first focused on the activity of neural units isolated from tetrodes located in the CA1 cell layer during the 4 h rest session (Fig. 2A.). We found no difference between groups in the number of neurons isolated during the 4 h rest period (Control (n=7) = 21.8 ± 5.5 cells, ArchT (n=6) = 20.3 ± 2.9 cells; P=0.83, unpaired t test). As prior work has suggested that the theta rhythm power during REMs may serve a homeostatic role by reducing overall firing rates while increasing ripple-associated neural synchrony observed during NREMs (*13*), we next analyzed these features from the last continuous 30 s period of NREMs prior to the first REMs episode as well as the first continuous 30 s periods of NREMs to follow the last REMs episode of the rest session (Fig. S2A.). We were unable to find a difference in NREMs firing rates (Fig. S2B.), nor in the proportion of ripple-coincident CA1 unit activity occurring during the same NREMs periods (Fig. S2D.), between the ArchT and Control groups. We next sought to determine whether a general disturbance in phase-locking of isolated neural activity to theta oscillations during REMs in the ArchT group could be behind the spatial memory deficits observed during the recall session in these mice (*11-12*). However, phase-locking of CA1 unit activity to theta oscillations was negligible in all groups (Fig. S2C.). Although the majority of REMs was characterized by sparse and uncoordinated CA1 neural activity with the exception of a relative minority of neurons occasionally exhibiting tonic activity, we consistently observed the presence of transient 'assemblies' ~10 ms in duration (Fig. 2B.). Thus, we next hypothesized that CA1 neural assemblies active during REMs could have a role in spatial memory formation which was disrupted in ArchT mice. We identified assembly events automatically by using a windowing-based approach to determine 10 ms segments of REMs with high levels of neural coactivity (*14*)(Fig. S3A-B, C (left).). The number of significant assembly activations occurring during REMs was reduced in the ArchT group versus controls, although not significantly (Fig. S3C, right.). However, synchrony analysis of neural activity occurring during assembly activations (*14*) revealed significantly lower (more synchronous) average values in the ArchT group relative to Controls (Fig. 2B-C.). Although the consistency of assembly compositions (constituent CA1 neurons) across REMs (via Pearson correlation analysis between binarized cell indice activity vectors (*14*)) was relatively strong for both the Control and ArchT conditions, suggesting relatively robust binding of a common subset of CA1 neurons to assemblies, it was significantly reduced for the ArchT condition relative to Control condition (Control (n=7) = 0.75 ± 0.4, ArchT (n=6) = 0.56 ± 0.03; P<0.0001, Mann Whitney test). We also wanted to investigate the characteristics of LFP activity occurring at the time of assembly activations. Wavelet power was calculated for 10 ms time windows centered around assembly activation time points (*14*) and averaged for each condition. Both ArchT and Control mice had activity peaks in the ~60-100 Hz range that was preferentially coupled to the theta trough (Fig. 2C, i,ii.). However, in addition to the characteristic reduction in theta power in ArchT mice, wavelet analysis further revealed the presence of prominent theta peak-associated activity in the ~30-60 Hz oscillation range during REMs assembly activity in these mice that was comparatively small in Controls (Fig. 2C, i,ii.), perhaps due to increased influence of intrahippocampal vs extrahippocampal gamma rhythm generators resulting from MSGABA inhibition (*16-17*). This may have promoted reduced synchrony of assembly activity relative to weaker oscillatory

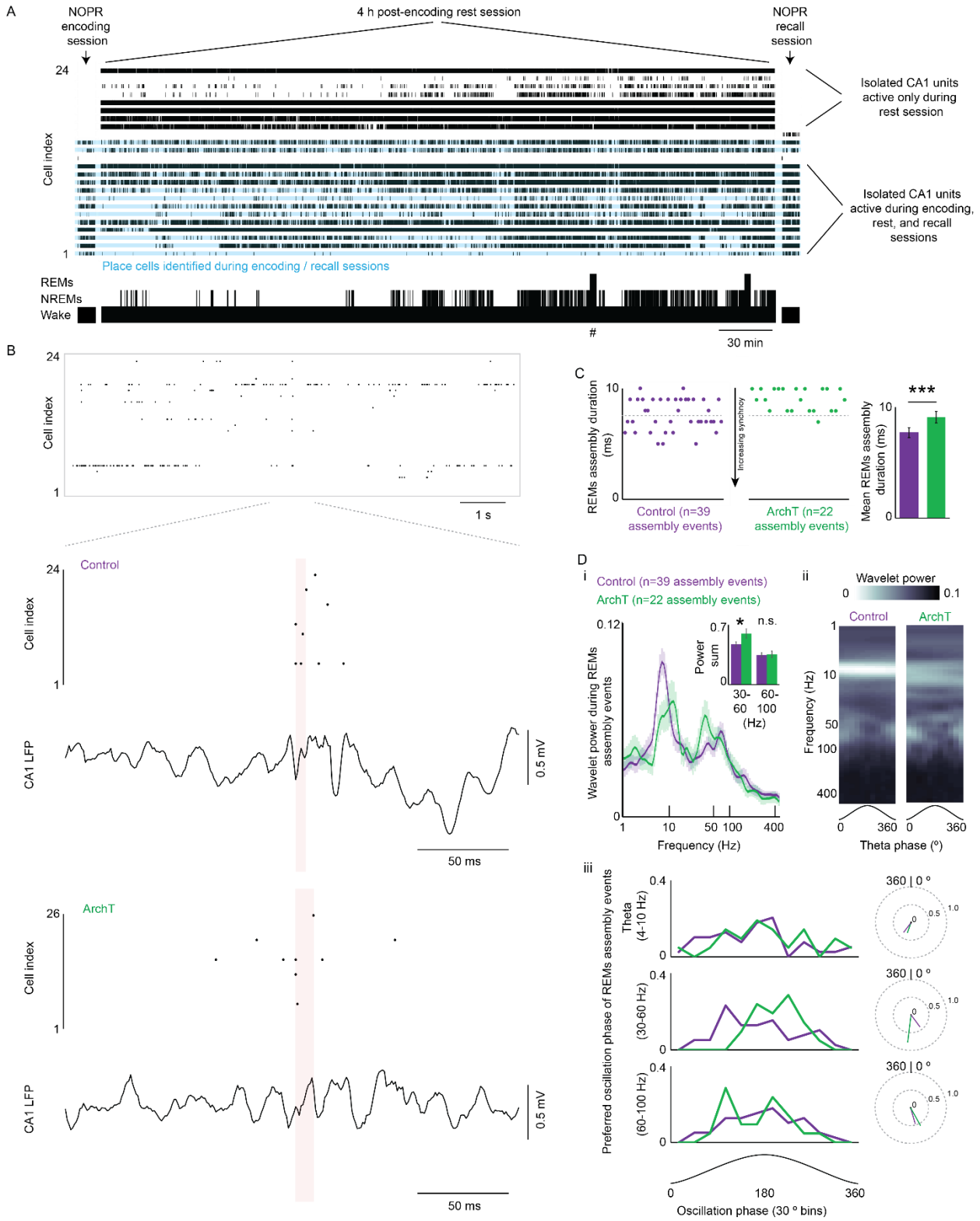
A
NOPR encoding session
4 h post-encoding rest session
NOPR recall session
Isolated CA1 units active only during rest session
Isolated CA1 units active during encoding, rest, and recall sessions
Cell index
Place cells identified during encoding / recall sessions
REMs
NREMs
Wake
30 min
B
Cell index
1 s
Control
ArchT
CA1 LFP
0.5 mV
50 ms
C
REMs assembly duration (ms)
Control (n=39 assembly events)
ArchT (n=22 assembly events)
Increasing synchrony
Mean REMs assembly duration (ms)
***
D
i
Control (n=39 assembly events)
ArchT (n=22 assembly events)
Wavelet power during REMs assembly events
Power sum
n.s.
(Hz)
Frequency (Hz)
ii
Wavelet power
Control
ArchT
Theta phase (°)
iii
Preferred oscillation phase of REMs assembly events
Theta (4-10 Hz)
(30-60 Hz)
(60-100 Hz)
Oscillation phase (30 ° bins)

Fig. 2. REMs-selective silencing of MSGABA reduces neural synchrony during CA1 assembly activity. (A) Example isolated CA1 unit recording (spike raster) from a single Control experiment. (B) Top. Spike raster centered around an example detected assembly occurring during the experiment shown in (A). The # symbol in (A) indicates the approximate location of the example detected assembly. Middle. High-resolution view of the detected assembly with the corresponding LFP trace below. The location and calculated duration (14) of the detected assembly is indicated by the pink shading. Bottom. Same as middle, except showing example data from a paired ArchT experiment. (C) Pooled analysis of REMs assembly durations during the rest session. (n=39 assemblies from 7 mice (Control), n=22 assemblies from 6 mice (ArchT); ***P<0.001, Mann Whitney test). (D) Analysis of LFP characteristics during REMs assembly activity. (i) Pooled wavelet power spectra calculated for a 10 ms window centered over REMs assembly activity during the rest session. Inset. Binned wavelet power for 30-60 Hz and 60-100 Hz bands. (n=39 assemblies from 7 mice (Control), n=22 assemblies from 6 mice (ArchT);*P<0.05, n=two-way ANOVA with Šídák's multiple comparisons test (ii) Average theta phase-amplitude coupling plots for Control vs. ArchT conditions, constructed by pooling phase-amplitude coupling data from the theta cycle coinciding with each detected REMs assembly. (iii) Pooled analysis of the preferred 4-10 Hz ('theta'), 30-60 Hz, and 60-100 Hz frequency oscillation phase of assembly activity during REMs. The corresponding mean vector length calculations are shown at right.

activity in the 60-100 Hz range that was present in both ArchT and Control mice, as phase-locking of assembly activity to ~30-60 Hz and ~60-100 Hz oscillatory activity was relatively strong and preferentially occurred at the peak in both Control and ArchT mice (Fig. 2C, iii.).

We next analyzed basic characteristics of CA1 place cells during the encoding and recall sessions, finding no difference between groups in the number of significant place cells identified (Control (n=7) = 12.7 ± 2.3 cells, ArchT (n=6) = 11.2 ± 2.3 cells; *P*=0.66, unpaired t test). All aforementioned identified place cells were also active during the intervening rest session (e.g., see Fig. 2A.). There were no consistent differences between groups in the mean values for key place cell characteristics (*14*)(Table S2.) for either the encoding or recall session. Place cell stability between the encoding and recall sessions (*14*) assessed through analysis of place field overlap (Control (n=37 place cells from 7 mice) = 0.42 ± 0.06, ArchT (n=41 place cells from 6 mice) = 0.32 ± 0.05; *P*=0.19, Mann Whitney test) and centroid displacement (Control (n=37 place cells from 7 mice) = 17.4 ± 2.8, ArchT (n=41 place cells from 6 mice) = 21.3 ± 2.3; *P*=0.12, Mann Whitney test), was also not found to differ between groups. We subsequently chose to concentrate on the subset of CA1 neurons which were active during REMs assemblies (18/37, 14/41 neurons used for stability analysis for Control and ArchT conditions, respectively), hypothesizing that the relative reduction in assembly synchrony in ArchT mice relative to Controls may have resulted in deficits in constituent place cell function during the recall session which were obscured in pooled data. We first calculated the basic properties of REMs assembly-active isolated CA1 neurons during the encoding and recall session, finding no consistent difference in these measures between groups (Table S3). However, the place field centroid shift was increased, and overlap proportion decreased, on average in REMs assembly-active place cells between the encoding and recall sessions in ArchT mice relative to Controls, indicating enhanced place cell stability in the latter (Fig. 3A-C.). This deficit was only found for REMs assembly-active CA1 neurons, as analysis of REMs assembly non-active CA1 neurons revealed relatively reduced place cell stability that was not different between groups. Population vector analysis of place cells (*14, 18-20*) revealed that these results manifested as a disruption of place cell activity at the population level in ArchT mice relative to Controls (Fig. 3D.).

Discussion

Cumulatively, our data provides mechanistic insight by suggesting that synchronous neural assemblies occurring in CA1 during REMs play a key role in spatial memory by promoting stabilization of the spatial representations of a subset of plastic neurons following encoding of spatial information. From a broader perspective, the relatively infrequent and transient nature of isolated CA1 neural assembly activity and general diversity in overt population-level CA1 neural activity patterns that we observed during REMs is consistent with it being a dynamic and heterogeneous behavioral state that has likely evolved to perform multiple functions (*21-25*), which could provide an explanation for recent seemingly contradictory results (*10, 26*).

Note that the schematics at top are only meant for illustrative purposes, and the object locations do not necessarily relate to the place field data below.

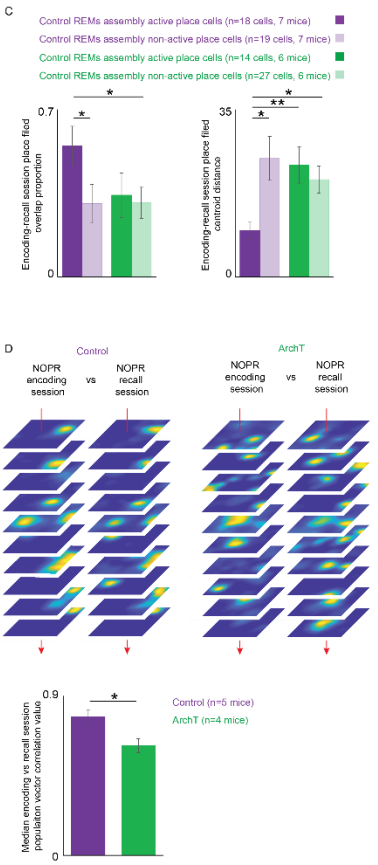

Fig. 3. MSGABA silencing during REMs reduces place cell stability in a subset of CA1 neurons. (A) Schematic demonstrating how 'REMs assembly active' and 'REMs assembly non-active' place cells were identified for stability analysis. Inset. High-resolution spike data (500 ms duration) centered around a single assembly activation during REMs. (B) Example of CA1 place fields calculated for the encoding and recall sessions. Values used to assess the stability of place fields across the two sessions (place field overlap and centroid displacement (14)) are included for each place cell at right. Max firing rates are indicated for each cell during the encoding and recall sessions by the value at top left of each corresponding rate map. (C) Left. Pooled place cell encoding-recall session overlap proportions. (n=18,19 cells from 7 mice (Control REMs active and Control REMs non-active conditions, respectively), n=14, 27 cells from 6 mice (ArchT REMs active and ArchT REMs non-active conditions, respectively); *P<0.05, Mann Whitney test). Right. Pooled encoding-recall session centroid distance. (n=18,19 cells from 7 mice (Control REMs active and Control REMs non-active conditions, respectively), n=14, 27 cells from 6 mice (ArchT REMs active and ArchT REMs non-active conditions, respectively); *P<0.05, **P<0.01, Mann Whitney test). (D) Place cell population vector analysis. Top. Schematic of the analysis procedure using sample data. Place fields calculated for the encoding and recall sessions from each mouse were stacked on top of each other. Population rate vectors, rate values obtained from each place field map at a given pixel, were then constructed for the encoding and recall sessions and directly compared via Pearson correlation (14). Bottom. Plot of the median correlation coefficient values obtained from this analysis. (n=5 (Control), n=4 (ArchT); *P<0.05, Mann Whitney test).

References and Notes

1. C. Grieser, R. Greenberg, R.H. Harrison, The adaptive function of sleep: the differential effects of sleep and dreaming on recall. J. Abnorm. Psychol. 80(3), 280-286 (1972).
2. G.J. Verschoor, T. Holdstock, REM bursts and REM sleep following visual and auditory learning. S. Afr. J. Psychol. 14(3), 69-74 (1984).
3. J. Buchegger, R. Fritsch, A. Meier-Koll, H, Riehle, Does trampolining and anaerobic physical fitness affect sleep? Percept. Mot. Skills. 73(1), 243-252 (1988).
4. Karni, D. Tanne, B.S. Rubenstein, J.J. Askenasy, D. Sagi, Dependence on REM sleep of overnight improvement of a perceptual skill. Science. 265(5172), 679-682 (1994).
5. Fogel, S.M., Smith, C.T. & Cote, K.A. Dissociable learning-dependent changes in REM and non-REM sleep in declarative and procedural memory systems. Behav Brain Res 180(1):48-61 (2007). 10.1016/j.bbr.2007.02.037.
6. C. Smith, K. Kitahama, J.L. Valatx, M Jouvet, Increased paradoxical sleep in mice during acquisition of a shock avoidance task. Brain. Res. 77(2), 221-230 (1974).
7. C. Smith, G. Kelly, Paradoxical sleep deprivation applied two days after end of training retards learning. Physiol. Behav. 43(2), 213-216 (1988).
8. C. Smith, G.M. Rose, Posttraining paradoxical sleep in rats is increased after spatial learning in the Morris water maze. Behav. Neurosci. 111(6), 1197-1204 (1997).

9. M. Aime, N. Calcini, M. Borsa, T. Campelo, T. Rusterholz, A. Sattin, T. Fellin, A. Adamantidis, Paradoxical somatodendritic decoupling supports cortical plasticity during REM sleep. Science. 376(6594), 724-730 (2022).

10. R. Boyce, S.D. Glasgow, S. Williams, A. Adamantidis, Causal evidence for the role of REM sleep theta rhythm in contextual memory consolidation. Science. 352(6287), 812-816 (2016).

11. G.R. Poe, D.A. Nitz, B.L. McNaughton, C.A. Barnes, Experience-dependent phase-reversal of hippocampal neuron firing during REM sleep. Brain. Res. 855(1), 176-180 (2000).

12. K. Mizuseki, K. Diba, E. Pastalkova, G. Buzsaki, Hippocampal CA1 pyramidal cells form functionally distinct sublayers. Nat. Neurosci. 14(9), 1174-1191 (2011).

13. A.D. Grosmark, K. Mizuseki, E. Pastalkova, K. Diba, G. Buzsaki, REM sleep reorganizes hippocampal excitability. Neuron. 75(6), 1001-1007 (2012).

14. Materials and methods are available as supplementary materials at the Science website.

15. M. Antunes, G. Biala, The novel object recognition memory: neurobiology, test procedure, and its modifications. Cognitive. Processing. 13, 93-110 (2012).

16. L.L. Colgin, Do slow and fast gamma rhythms correspond to distinct functional states in the hippocampal network? Brain. Res. 1621, 309-315 (2015).

17. L.L. Colgin, T. Denninger, M. Fyhn, T. Hafting, T. Bonnvie, O. Jensen, M-B. Moser, E.I. Moser, Frequency of gamma oscillations routes flow of information in the hippocampus. Nature. 462, 353-357 (2009).

18. D. Dupret, J. O'Neill, B. Pleydell-Bouverie, J. Csicsvari, The reorganization and reactivation of hippocampal maps predict spatial memory performance. Nat. Neurosci. 13, 995-1002 (2010).

19. E.A. Mankin, F.T. Sparks, B. Slayyeh, R.J. Sutherland, S. Leutgeb, J.K. Leutgeb, Neuronal code for extended time in the hippocampus. Proc. Natl. Acad. Sci. U. S. A. 109(47), 19462-19467 (2012).

20. L. Roux, B. Hu, R. Eichler, E. Stark, G. Buzsaki, Sharp wave ripples during learning stabilize hippocampal spatial map. Nat. Neurosci. 20(6), 845-853 (2017).

21. J.M. Siegel, M.A. Rogawski, A function for REM sleep: regulation of noradrenergic receptor sensitivity. Brain. Res. 472(3), 213-233 (1988).

22. G.A. Marks, J.P. Shaffery, A. Oksenberg, S.G. Speciale, H.P. Roffwarg, A functional role for REM sleep in brain maturation. Behav. Brain. Res. 69(1-2), 1-11 (1995).

23. J.A. Hobson, REM sleep and dreaming: towards a theory of protoconsciousness. Nat. Rev. Neurosci. 10(11), 803-813 (2009).

24. L. Wei, L. Ma, G. Yang, W-B. Gan, REM sleep selectively prunes and maintains new synapses in development and learning. Nat. Neurosci. 20(3):427-437 (2017).

25. O.I. Lyamin, P.O. Kosenko, S.M. Korneva, A.L. Vyssotski, L.V. Mukhametov, J.M. Siegel, Fur seals suppress REM sleep for very long periods without subsequent rebound. Curr. Biol. 28(12), 2000-2005 (2018).

26. S. Izawa, S. Chowdhury, T. Miyazaki, Y. Mukai, D. Ono, R. Inoue, Y. Ohmura, H. Mizoguchi, K. Kimura, M. Yoshioka, A. Terao, T. Kilduff, A. Yamanaka, REM sleep-active MCH neurons are involved in forgetting hippocampus-dependent memories. Science. 365(6459), 1308-1313 (2019).

27. T.F. Freund, M. Antal, GABA-containing neurons in the septum control inhibitory interneurons in the hippocampus. Nature. 336(6195), 170-173 (1988).

28. H. Bokil, P. Andrews, J.E. Kulkarni, S. Mehta, P.P. Mitra, Chronux: a platform for analyzing neural signals. J. Neurosci. Methods. 192(1), 146-151 (2010).

29. A.G. Siapas, M.A. Wilson, Coordinated interactions between hippocampal ripples and cortical spindles during slow-wave sleep. Neuron. 21(5), 1123-1128 (1998).

30. W.E. Skaggs, B.L. McNaughton, M.A. Wilson, C.A. Barnes, Theta phase precession in hippocampal neuronal populations and the compression of temporal sequences. Hippocampus. 6, 149-172 (1996).